A Cramer–Rao Lower Bound of CSI-Based Indoor Localization

Linqing Gui, Mengxia Yang, Hai Yu, Jun Li, Feng Shu, and Fu Xiao

***Abstract*—Due to robustness against multipath effect, frequency domain CSI (Channel State Information) of OFDM (Orthogonal Frequency Division Multiplexing) systems is supposed to provide good ranging measurement for indoor localization. Since lower bound of positioning error for CSI-based localization has been rarely reported, this paper proposes a Cramer–Rao lower bound (CRLB) for CSI-based localization. This CRLB is derived based on indoor wireless propagation model integrating both shadowing effect and multipath effect. The main factors that can influence the CRLB are analyzed. Through simulations and analysis, the gap between CSI-based localization error and the proposed CRLB is presented, and the influence by three main factors is thoroughly investigated.**

***Index Terms*—Channel state information, orthogonal frequency division multiplexing, indoor localization, Cramer–Rao lower bound.**

I. Introduction

Localization is one important module in a wide range of wireless applications such as indoor navigation, surveillance and mobile crowd-sensing [1]–[4]. Although Global Positioning System (GPS) is a popular outdoor localization technique, it does not perform well in indoor environment because satellite signals can hardly penetrate concrete walls and roofs [5], [6]. Moreover, GPS has additional hardware cost and consumes more energy. Therefore, GPS-free techniques are required for indoor localization.

A large number of indoor localization methods have been proposed these years. They can be divided into two categories: range-based and range-free. Rather than range-free methods, range-based ones are usually preferred because of their better accuracy. This is achieved through distance (or direction) ranging measurement between target mobile device and each anchor. Traditional ranging measurements include RSS (Received Signal Strength), TOA (Time of Arrival), TDOA (Time Difference of Arrival) and AOA (Angle of Arrival).

CSI (Channel State Information) of OFDM (Orthogonal Frequency Division Multiplexing) systems provides a new low-cost ranging measurement [7]. Due to high frequency efficiency and robustness against multi-path effect [8], OFDM has been widely used in broadband wireless communication systems such as LTE (Long Term Evolution) and WiFi (Wireless Fidelity). The recent WiFi standards IEEE 802.11a/g/n/ac all support OFDM. With the vast use of OFDM, the frequency-domain CSI can be obtained without additional hardware [9]. Thus the hardware cost of CSI-based localization can be as low as RSS-based method. Furthermore, less influenced by multi-path effect, the stability of CSI is much better than RSS [8], [10]. Therefore CSI-based localization is supposed to achieve good accuracy with low cost.

CSI-based localization was first proposed by Wu *et al.* [7]. The authors proposed two ways to exploit CSI to fulfill localization. One is to use CSI to estimate distance through propagation model, while the other is to find the matched position in a CSI-based fingerprinting system. In this paper we mainly focus on the former way, i.e., CSI-based localization through propagation model. Although several new algorithms such as PhaseU [11] and PhaseFi [12] were proposed to improve the original CSI-based localization, to the best of our knowledge, research on lower bound of CSI-based localization error has not been reported. Thus the main contributions of this paper include:

1) A Cramer-Rao lower bound (CRLB) on CSI-based localization error has been derived. This lower bound *provides a reference on the best accuracy that the most accurate CSI-based localization method could achieve or approach*. To the best of our knowledge, this is the first paper about CRLB on CSI-based localization. Since shadowing and multi-path fading are two main error resources for CSI-based localization, they are both taken into consideration for the derivation of CRLB.
2) Through simulations and analysis, the influence by some main factors (such as the bandwidth, the number of anchors and the shadowing effect) is thoroughly investigated for both CSI-based localization error and the proposed CRLB.

The remainder of this paper is organized as follows. The system model is introduced in Section II. We derive a Cramer-Rao lower bound in Section III. Simulation and analysis are presented in Section IV. Section V concludes this paper.

II. System Model

A. Wireless Propagation Model

In wireless communication, the attenuation of signal strength through a radio channel is mainly caused by three factors: path loss, shadowing and multipath fading [13]. To characterize multipath propagation, the wireless channel can be modeled as a temporal linear filter, known as Channel Impulse Response (CIR). Under the time-invariant assumption *[9]*, CIR (without consideration of noise) can be

Manuscript received May 13, 2017; revised September 26, 2017; accepted November 9, 2017. Date of publication November 15, 2017; date of current version March 15, 2018. This work was supported in part by the National Natural Science Foundation of China under Grants 61602245, 61771244, 61501238, and 61702258, in part by the Nature Science Foundation of Jiangsu for Distinguished Young Scientist under Grant BK20170039, in part by the Natural Science Foundation of Jiangsu Province under Grants BK20150791 and BK20150786, in part by Fundamental Research Funds for the Central Universities under Grant 30916011205, and in part by Open Research Fund of National Mobile Communications Research Laboratory Southeast University under Grant 2017D04. The review of this paper was coordinated by Dr. J. Wang. *(Corresponding author: Fu Xiao.)*

L. Gui, M. Yang, H. Yu, J. Li, and F. Shu are with the Department of Electronic and Optical Engineering, Nanjing University of Science and Technology, Nanjing 210094, China (e-mail: guilinqing@gmail.com; 597990359@qq.com; 40776838@qq.com; jun.li@njust.edu.cn; shufeng0101@163.com).

F. Xiao is with the College of Computer, Nanjing University of Posts and Telecommunications, Nanjing 210003, China (e-mail: xiaof@njupt.edu.cn).

Color versions of one or more of the figures in this paper are available online at http://ieeexplore.ieee.org.

Digital Object Identifier 10.1109/TVT.2017.2773635

denoted as:

$$h(t) = \sum_{m=0}^{M} \alpha_m e^{-j\theta_m} \delta(t - \tau_m) \quad (1)$$

where $\delta(t)$ is the Dirac delta function. In total there are $M + 1$ paths including one *Line of Sight (LOS)* path and M NLOS paths. α_m, θ_m, and τ_m represent the amplitude, phase, and delay of the m-th path respectively, while α_0 denotes the attenuation amplitude of the LOS path. Since the attenuation of signal strength along the LOS path is mainly caused by path loss and shadowing [13], α_0 can be expressed as:

$$\alpha_0 = \frac{\lambda\sqrt{G_t G_r}}{(4\pi d_0)^{n/2}} A_0 \quad (2)$$

where λ is the wavelength of the transmitted signal, G_r and G_t are respectively the antenna gains at the receiver and transmitter, d_0 denotes the distance of the LOS path, n is the environmental attenuation factor, and A_0 represents the attenuation of signal amplitude caused by shadowing.

The NLOS paths originate from radio reflection and refraction. During each reflection or refraction, only partial energy of the signal is transmitted [14], which can be measured by a reflection/refraction coefficient ε. Therefore, base on (2), with the reflection/refraction coefficient, the amplitude of the m-th path α_m can be expressed as

$$\alpha_m = \frac{\lambda\sqrt{G_t G_r}}{(4\pi d_m)^{n/2}} A_m \varepsilon^{l_m} \quad (3)$$

where the reflection/refraction coefficient $\varepsilon \in (0, 1)$. The number of reflections (or refractions) along the m-th path is l_m and each reflection/refraction is assumed to have the same coefficient. d_m is the distance of the m-th NLOS path. A_m denotes the attenuation of signal amplitude caused by shadowing along the m-th path. Therefore, based on the (1)–(3), a simplified wireless propagation model is built, integrating the effects of path loss, shadowing and multi-path.

B. CSI-Based Localization Model

In OFDM systems, CSI represents the measurement of the amplitudes and phases of channel frequency response (CFR) on each subcarrier. Thus each CSI can be expressed as:

$$H(f_k) = |H(f_k)|e^{j\theta_k} \quad (4)$$

where $H(f_k)$ is the CSI at the subcarrier of central frequency f_k, $|H(f_k)|$ is the amplitude, and θ_k is the phase. A set of CSIs $\{H(f_k)$ $(k = 1, \ldots, K)\}$ represent K sampled CFRs.

Rather than directly use these CSIs, the original CSI-based localization method [7] first converts the CSIs into time domain by Inverse Fast Fourier Transform (IFFT), obtains the samples of channel impulse response (CIR), then uses a threshold-based method to filter *the CIRs containing the LOS path (if exists) and the shortest NLOS path (the shortest reflection path with the smallest time delay)*. The filtered CIRs are once again converted into frequency domain by Fast Fourier Transform (FFT), thus a new set of filtered CSIs denoted as $\widetilde{H}(f_k)$ $(k = 1, \ldots, K)$ can be obtained. In order to compensate frequency-selective fading, the amplitude of the new set of CSIs is combined through weighted averaging. The combination result named as the effective CSI is calculated as

$$CSI_{\text{eff}} = \frac{1}{K} \sum_{k=1}^{K} \frac{f_k}{f_c} |\widetilde{H}(f_k)| \quad (5)$$

where f_c is the central frequency of the whole band.

By revising the free space propagation model, the distance between mobile device and one anchor is estimated as

$$d = \frac{1}{4\pi} \left[\left(\frac{c}{f_c \times CSI_{\text{eff}}} \right)^2 \times \sigma \right]^{\frac{1}{n}} \quad (6)$$

where c is the radio velocity, n is the path loss attenuation factor, and σ is the environment factor. In fact, both n and σ depend on indoor environments. These two parameters are retrieved for each anchor through a simple supervised learning method. Finally, with the estimated distances to all anchors, mobile device can calculate its position by multi-lateration.

III. A Cramer-Rao Lower Bound on Location Error of CSI-Based Localization

First, CSI can be derived based on the wireless channel propagation model given in section II.A. Since CFR can be obtained through the Fourier transform of channel impulse response, the CFR corresponding to (1) is

$$H(\omega) = \text{FourierTransform}[h(t)] = \sum_{m=0}^{M} \alpha_m \cdot e^{-j(\omega\tau_m + \theta_m)} \quad (7)$$

Substituting $e^{-j(\omega\tau_m + \theta_m)}$ with $\cos(\omega\tau_m + \theta_m) - j\sin(\omega\tau_m + \theta_m)$, we can express CSI as

$$H(f_k) = \sum_{m=0}^{M} \alpha_m \cos\phi_m - j \sum_{m=0}^{M} \alpha_m \sin\phi_m \quad (8)$$

where $\phi_m = 2\pi f_k \tau_m + \theta_m$, and $k \in \{1, ..., K\}$ if the whole band of OFDM system is divided into K subcarriers (normally K is an even number).

The original CSI-based localization needs to convert the CSIs into a new set of filtered CSIs. This new set of CSIs denoted as $\widetilde{H}(f_k)$ has similar expression as $H(f_k)$ in (8). The difference between $\widetilde{H}(f_k)$ and $H(f_k)$ lies on the number of multi-path components. If the number of NLOS paths for $\widetilde{H}(f_k)$ is denoted as $\overline{M}$, then $\widetilde{H}(f_k)$ can be expressed as

$$\widetilde{H}(f_k) = \sum_{m=0}^{\overline{M}} \alpha_m \cos\phi_m - j \sum_{m=0}^{\overline{M}} \alpha_m \sin\phi_m \quad (9)$$

Theoretically if the time resolution of the system is so high that the LOS path or the shortest NLOS path can be distinguished, $\overline{M}$ could be as small as 0 or 1. However, as mentioned in [7], due to the limited bandwidth of WLAN, the time resolution is limited, and it is impossible to distinguish all the reflection paths. Instead, with limited time resolution, clusters of reflection paths can be distinguished. The original CSI-based localization method filters the first cluster of CIR, because the first cluster is supposed to contain the LOS path or the shortest NLOS path. Therefore $\overline{M}$ equals to the number of reflection paths in the first cluster.

Then based on (5), the effective CSI can be calculated

$$CSI_{\text{eff}} = \frac{1}{K}\sum_{k=1}^{K}\frac{f_k}{f_c}\left(\left(\sum_{m=0}^{\overline{M}}\alpha_m\cos\left(2\pi f_k\tau_m+\theta_m\right)\right)^2 + \left(\sum_{m=0}^{\overline{M}}\alpha_m\sin\left(2\pi f_k\tau_m+\theta_m\right)\right)^2\right)^{\frac{1}{2}} \tag{10}$$

Though some accuracy is sacrificed, the square of CSI_{eff} can be approximated by a weighted sum of square expressions:

$$CSI_{\text{eff}}^2 \approx \sum_{k=1}^{K}\frac{f_k}{Kf_c}\left(\left(\sum_{m=0}^{\overline{M}}\alpha_m\cos\left(2\pi f_k\tau_m+\theta_m\right)\right)^2 + \left(\sum_{m=0}^{\overline{M}}\alpha_m\sin\left(2\pi f_k\tau_m+\theta_m\right)\right)^2\right) \tag{11}$$

According to the analysis in [15], when l_m is more than 1, the radio along the m-th path is reflected (or refracted) multiple times, then ε^{l_m} becomes very small. Besides, multiple reflections or refractions always significantly increase the distance of the m-th path. Thus the signal received from the m-th path has minimal contribution to the total received power. Therefore l_m can be limited to 1.

Since α_0 and α_m $(m>0)$ have different expressions as shown respectively in (2) and (3), all the amplitudes in (11) can be separated to α_0 and α_m $(m>0)$. Besides, θ_m equals to $2\pi f_k\tau_m$ [13], while d_m equals to $c(\tau_m-\tau_0)+d_0$. Therefore, based on (2) and (3), if the antenna gains G_t and G_r are assumed to be 1, (11) can further expand as

$$CSI_{\text{eff}}^2 = \frac{c^2}{{f_c}^2(4\pi d_0)^n}\sum_{k=1}^{K}\frac{f_k}{Kf_c}\left\{A_0^2+\sum_{m=1}^{\overline{M}}\frac{A_m^2\varepsilon^2}{\left(1+\frac{c(\tau_m-\tau_0)}{d_0}\right)^n} + \sum_{m=1}^{\overline{M}}\frac{2A_0A_m\varepsilon\cos\left[4\pi f_k(\tau_m-\tau_0)\right]}{\left(1+\frac{c(\tau_m-\tau_0)}{d_0}\right)^{n/2}} + \sum_{m=1}^{\overline{M}-1}\sum_{p=m+1}^{\overline{M}}\frac{2A_mA_p\varepsilon^2\cos\left[4\pi f_k(\tau_m-\tau_p)\right]}{\left(\left(1+\frac{c(\tau_m-\tau_0)}{d_0}\right)\left(1+\frac{c(\tau_p-\tau_0)}{d_0}\right)\right)^{n/2}}\right\} \tag{12}$$

From the comparison between (12) and (6), it can be found that (6) could be derived from (12) with the requirement of the following two assumptions. The first assumption is that multi-path effects could be completely mitigated. With this assumption, the number of NLOS paths becomes 0. The second assumption is that A_0^2 equals to the environment factor σ. In fact, the relation between these two parameters was mentioned in [7], as the power loss due to shadowing was included in the environment parameter σ. However, it should be noted that in practice, rather than the shadowing effect along the path between mobile device and each anchor, it is the shadowing power loss between anchors that is included in σ, because σ is estimated in offline *phase* by using training data along the path between the anchors [7].

The effective CSI calculated in (12) refers to the channel status between mobile device and one anchor. The subscript i used to denote the i-th anchor, (12) can be written as

$$CSI_{\text{eff},i}^2 = \frac{c^2\sigma}{{f_c}^2(4\pi d_{0,i})^n}\sum_{k=1}^{K}\frac{f_k}{Kf_c}\left\{\frac{A_{0,i}^2}{\sigma}+\sum_{m=1}^{\overline{M}}\frac{A_{m,i}^2\varepsilon^2}{\sigma\left(1+\frac{c(\tau_{m,i}-\tau_{0,i})}{d_{0,i}}\right)^n} + \sum_{m=1}^{\overline{M}}\frac{2A_{0,i}A_{m,i}\varepsilon\cos\left[4\pi f_k(\tau_{m,i}-\tau_{0,i})\right]}{\sigma\left(1+\frac{c(\tau_{m,i}-\tau_{0,i})}{d_{0,i}}\right)^{n/2}} + \sum_{m=1}^{\overline{M}-1}\sum_{p=m+1}^{\overline{M}}\frac{2A_{m,i}A_{p,i}\varepsilon^2\cos\left[4\pi f_k(\tau_{m,i}-\tau_{p,i})\right]}{\sigma\left(\left(1+\frac{c(\tau_{m,i}-\tau_{0,i})}{d_{0,i}}\right)\left(1+\frac{c(\tau_{p,i}-\tau_{0,i})}{d_{0,i}}\right)\right)^{n/2}}\right\} \tag{13}$$

The logarithm form of (13) can be expressed as

$$v_i = L(d_{0,i})+\eta_i \tag{14}$$

where

$$v_i = \ln CSI_{\text{eff},i}^2 \tag{15}$$

$$L(d_{0,i}) = \ln\frac{c^2\sigma}{{f_c}^2(4\pi d_{0,i})^n} \tag{16}$$

and

$$\eta_i = \ln\left\{\frac{A_{0,i}^2}{\sigma}+\sum_{m=1}^{\overline{M}}\frac{A_{m,i}^2\varepsilon^2}{\sigma\left(1+\frac{c(\tau_{m,i}-\tau_{0,i})}{d_{0,i}}\right)^n} + \sum_{k=1}^{K}\sum_{m=1}^{\overline{M}}\frac{2f_kA_{0,i}A_{m,i}\varepsilon\cos\left[4\pi f_k(\tau_{m,i}-\tau_{0,i})\right]}{Kf_c\sigma\left(1+\frac{c(\tau_{m,i}-\tau_{0,i})}{d_{0,i}}\right)^{n/2}} + \sum_{k=1}^{K}\sum_{m=1}^{\overline{M}-1}\sum_{p=m+1}^{\overline{M}}\frac{2f_kA_{m,i}A_{p,i}\varepsilon^2\cos\left[4\pi f_k(\tau_{m,i}-\tau_{p,i})\right]}{Kf_c\sigma\left(\left(1+\frac{c(\tau_{m,i}-\tau_{0,i})}{d_{0,i}}\right)\left(1+\frac{c(\tau_{p,i}-\tau_{0,i})}{d_{0,i}}\right)\right)^{n/2}}\right\} \tag{17}$$

From (14), it can be observed that the measured effective CSI is a combination of CSI-ranging model as (6) and a random variable η_i. Since (6) is the basic ranging model for the original CSI-based localization, η_i can be regarded as measurement noise. Here η_i is a random variable because both the shadowing-related power loss $A_{m,i}$ and the NLOS-path propagation delay $\tau_{m,i}$ are random variables.

If the unknown position of mobile device and the position of the i-th anchor are denoted as $\psi=(x,y)^T$ and $\psi_i=(x_i,y_i)^T$ respectively, then the LOS distance between the mobile device and the i-th anchor can be calculated as $d_{0,i}=\sqrt{(\psi-\psi_i)^T(\psi-\psi_i)}$. Since $d_{0,i}$ is a function of ψ, $L(d_{0,i})$ can also be expressed as a function of ψ, i.e., $L_i(\psi)$. Then we can turn (14) into

$$\eta_i = v_i - L(d_{0,i}) \tag{18}$$

If η_i is assumed as a normal random variable with mean 0 and variance $\sigma_{\eta_i}^2$, then the probability density function (PDF) of v_i is

$$f_v(v_i;\psi) = \frac{1}{\sqrt{2\pi}\sigma_{\eta_i}}\exp\left(\frac{-\left(v_i-L_i(\psi)\right)^2}{2\sigma_{\eta_i}^2}\right) \tag{19}$$

Let $v=(v_1,v_2,...,v_{Na})$ denote the vector of effective CSIs measured at mobile device for all anchors. The number of anchors is N_a.

It is assumed that the elements in the vector v are independent and identically distributed. Then, we have the logarithm of the joint PDF $\ln f_v(v;\psi)$ as

$$\ln f_v(v;\psi) = -\sum_{i=1}^{Na} \frac{1}{2\sigma_{\eta_i}^2}\left(v_i - L_i(\psi)\right)^2 + \sum_{i=1}^{Na} \ln \frac{1}{\sqrt{2\pi}\sigma_{\eta_i}} \quad (20)$$

The Fisher information matrix (FIM) [16] is given by

$$[F(\psi)]_{kl} = -E\left[\frac{\partial^2 \ln f_v(v;\psi)}{\partial\psi_k \partial\psi_l}\right] \quad (21)$$

Then the Cramer-Rao lower bound (CRLB) of mean square error of ψ can be calculated as

$$CRLB = \frac{[F(\psi)]_{11} + [F(\psi)]_{22}}{[F(\psi)]_{11}[F(\psi)]_{22} - [F(\psi)]_{12}^2} \quad (22)$$

where

$$[F(\psi)]_{11} == \sum_{i=1}^{Na} \frac{1}{\sigma_{\eta_i}^2}\left(\frac{n(x-x_i)}{d_{0,i}^2}\right)^2 \quad (23)$$

$$[F(\psi)]_{22} = \sum_{i=1}^{Na} \frac{1}{\sigma_{\eta_i}^2}\left(\frac{n(y-y_i)}{d_{0,i}^2}\right)^2 \quad (24)$$

$$[F(\psi)]_{12} = \sum_{i=1}^{Na} \frac{1}{\sigma_{\eta_i}^2}\left(\frac{n^2(x-x_i)(y-y_i)}{d_{0,i}^4}\right) \quad (25)$$

From the derivation result of CRLB, it can be observed that lower bound of CSI-based localization error is mainly influenced by $\sigma_{\eta_i}^2$ and $d_{0,i}$. Since $\sigma_{\eta_i}^2$ is the variance of η_i which is the measurement noise of effective CSI between mobile device and each anchor, those factors in the expression of η_i in (17) can also have impact on the derived CRLB. Therefore, the CRLB of CSI-based localization error can be influenced by multiple factors such as the distance to each anchor, the number of subcarriers, the frequencies of subcarriers, the path loss attenuation factor n, the shadowing effect and multi-path effect. Specifically, the factor related to shadowing effect can be represented by σ_s^2 which is the variance of power attenuation due to shadowing. The factors related to multi-path effect include the number of NLOS paths $\overline{M}$, the delay of each path $\tau_{m,i}$ and the reflection/refraction coefficient ε.

IV. Simulation and Analysis

In this section, using MATLAB we simulate the original CSI-based localization method and compare its accuracy with the proposed CRLB. The scenario is set inside a 10 m × 10 m indoor office. The indoor radio propagation model used in the simulation has been introduced in the Section II-B, integrating shadowing effect and multi-path effect. The main parameters in the simulation are listed in Table I.

We consider three main factors that can influence CSI-localization error, i.e., the number of anchors (N_a), the bandwidth and the variance of power-loss due to shadowing (σ_s^2). When observing how location error behaves with the change of one particular factor, we fix all other factors as their default values, then run the simulation as many as 5000 times. Each time the target mobile device is randomly deployed, while the anchors locate on the borders sparsely.

As shown in Fig. 1, CSI-based localization error is compared with *the root of average CRLB* under different number of anchors. For the convenience of observation, the scale of y-axis is set to be logarithmic. In Fig. 1, it can be observed that when the number of anchors increases, the location error of CSI-based localization decreases as well as the proposed CRLB. The reason is that more positioning information can be obtained when more anchors join to help localize the target device. It can also be observed that under the same number of anchors, the root of CRLB is much smaller than the CSI-based localization error. One main reason for this gap lies on the estimation bias of path loss attenuation factor n and environment factor σ in (6). *Theoretically, these two parameters should be estimated based on the radio propagation environment along the path between target device and each anchor. However, in practice this cannot be fulfilled because the position of target device is to be decided. Alternatively these two parameters are estimated at offline stage along the path between anchors.* This brings estimation error into n and σ. Then at online stage this error passed through (6) and becomes one main source error for CSI-based localization.

Under different bandwidth, the CSI-based localization error is compared with the root of proposed CRLB as shown in Fig. 2. In the simulation, since the bandwidth of each subcarrier is fixed, the change of whole bandwidth is equivalent to the change of the number of subcarriers. In Fig. 2, when the bandwidth gets larger, the location error obviously becomes smaller. The reason is that with larger bandwidth, the time resolution becomes higher, then more multi-path components are filtered out in the effective CSI. In Fig. 2, it can also be observed that when the bandwidth increases, the change of the proposed CRLB is not

TABLE I
Main Parameters in the Simulation

Parameter	Value
N_a	range from 3 to 8; default value is 3.
n	range from 2 to 5; default value is 2.
${\sigma_s}^2$	range from 1 to 5; default 5.
M	50
$d_{0,i}$ (m)	random between 1 and 15
distance of NLOS path (m)	random between $1.2d_{0,i}$ and 20
ε	0.3
K	64, 128, 256, 512 or 1024; default 64.
Bandwidth (MHz)	20, 40, 80, 160 or 320; default 20.
modulation scheme	16QAM
the center frequency f_c	5 GHz (as in IEEE 802.11a)

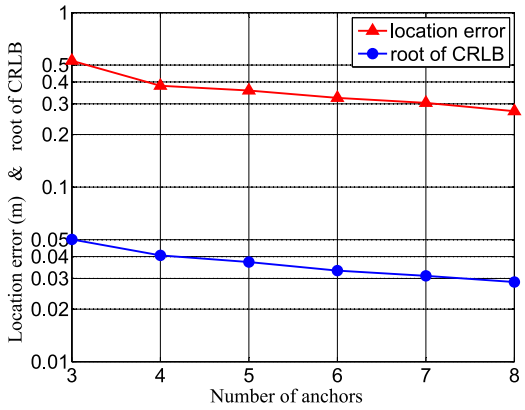

Fig. 1. Comparison under different number of anchors.

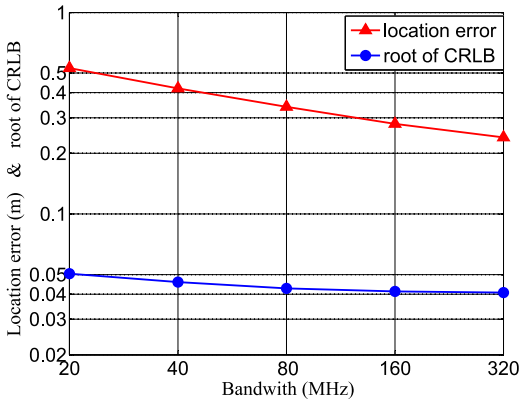

Fig. 2. Comparison under different bandwidth.

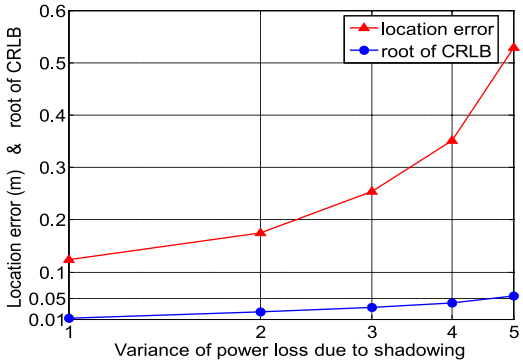

Fig. 3. Comparison under different variance of power attenuation due to shadowing.

so significant as that of the location error. It indicates that increasing the bandwidth could be an effective way to narrow the gap between location error and the CRLB.

As shown in Fig. 3, CSI-based localization error is compared with the root of proposed CRLB under different variance of shadowing-related power attenuation. It can be observed that as the variance σ_s^2 gets bigger, the location error of CSI-based localization becomes larger as well as the proposed CRLB. The reason is the influence of shadowing effect. A bigger variance σ_s^2 indicates a stronger shadowing effect which brings larger fluctuation to the effective CSI.

V. Conclusion

This paper proposes a Cramer-Rao lower bound on positioning error of CSI-based indoor localization. This CRLB is derived based on indoor wireless propagation model integrating both shadowing effect and multi-path effect. The derivation result shows that the CRLB on CSI-based localization error can be influenced by multiple factors such as the distance between target device and each anchor, the number and frequencies of subcarriers, the path loss attenuation factor, the shadowing effect and multi-path effect. Specifically, the factors related to multi-path effect include the number of NLOS paths, the delay of each path and the reflection/refraction coefficient, while the factor related to shadowing effect is represented by the variance of power attenuation due to shadowing. Through simulations and analysis, CSI-based localization error and the proposed CRLB are compared, and the influence by three main factors has been investigated. Simulation results show that both CSI-based localization error and the proposed CRLB decrease with more anchors, larger bandwidth or smaller variance of shadowing-related power attenuation. It is also observed that increasing the bandwidth could be a practical method to narrow the gap between location error and CRLB.

References

[1] Z. Yin, C. Wu, Z. Yang, and Y. Liu, "Peer-to-peer indoor navigation using smartphones," *IEEE J. Sel. Areas Commun.*, vol. 35, no. 5, pp. 1141–1153, May 2017.

[2] S. He, D. H. Shin, J. Zhang, J. Chen, and Y. Sun, "Full-view area coverage in camera sensor networks: Dimension reduction and near-optimal solutions," *IEEE Trans. Veh. Technol.*, vol. 65, no. 9, pp. 7448–7461, Sep. 2016.

[3] X. Zhang *et al.*, "Incentives for mobile crowd sensing: A survey," *IEEE Commun. Surveys Tut.*, vol. 18, no. 1, pp. 54–67, First Quarter 2016.

[4] X. Duan, C. Zhao, S. He, P. Cheng, and J. Zhang, "Distributed algorithms to compute walrasian equilibrium in mobile crowdsensing," *IEEE Trans. Ind. Electron.*, vol. 64, no. 5, pp. 4048–4057, May 2017.

[5] L. Shangguan, Z. Yang, A. X. Liu, Z. Zhou, and Y. Liu, "Stpp: Spatial-temporal phase profiling-based method for relative RFID tag localization," *IEEE/ACM Trans. Netw.*, vol. 25, no. 1, pp. 596–609, Feb. 2017.

[6] F. Xiao, Z. Wang, N. Ye, R. Wang, and X. Li, "One more tag enables fine-grained RFID localization and tracking," *IEEE/ACM Trans. Netw.*, vol 26, no. 1, pp. 161–174, Feb. 2018.

[7] K. Wu, J. Xiao, Y. Yi, D. Chen, X. Luo, and L. M. Ni, "Csi-based indoor localization," *IEEE Trans. Parallel Distrib. Syst.*, vol. 24, no. 7, pp. 1300–1309, Jul. 2013.

[8] H. Zhu and J. Wang, "Chunk-based resource allocation in OFDMA systems—Part II: Joint chunk, power and bit allocation," *IEEE Trans. Commun.*, vol. 60, no. 2, pp. 499–509, Feb. 2012.

[9] Z. Yang, Z. Zhou, and Y. Liu, "From RSSI to CSI, Indoor localization via channel response," *ACM Comput. Surveys*, vol. 46, no. 2, pp. 25:1–25:32, Dec. 2013.

[10] H. Zhu, F. Xiao, L. Sun, R. Wang, and P. Yang, "R-ttwd: Robust device-free through-the-wall detection of moving human with wifi," *IEEE J. Sel. Areas Commun.*, vol. 35, no. 5, pp. 1090–1103, May 2017.

[11] C. Wu, Z. Yang, Z. Zhou, K. Qian, Y. Liu, and M. Liu, "Phaseu: Real-time los identification with wifi," in *Proc. 2015 IEEE Conf. Comput. Commun.*, Apr. 2015, pp. 2038–2046.

[12] X. Wang, L. Gao, and S. Mao, "CSI phase fingerprinting for indoor localization with a deep learning approach," *IEEE Internet Things J.*, vol. 3, no. 6, pp. 1113–1123, Dec. 2016.

[13] D. Tse and P. Viswanath, *Fundamentals of Wireless Communication*. Cambridge, U.K.: Cambridge Univ. Press, 2005.

[14] C. A. Balanis, *Antenna Theory: Analysis and Design*. Hoboken, NJ, USA: Wiley, 2016.

[15] X. Guo, D. Zhang, K. Wu, and L. M. Ni, "Modloc: Localizing multiple objects in dynamic indoor environment," *IEEE Trans. Parallel Distrib. Syst.*, vol. 25, no. 11, pp. 2969–2980, Nov. 2014.

[16] F. Shu, S. Yang, Y. Qin, and J. Li, "Approximate analytic quadratic-optimization solution for tdoa-based passive multi-satellite localization with earth constraint," *IEEE Access*, vol. 4, pp. 9283–9292, 2016.